

Effect of lipid rafts on ligand dissociation: enhanced rebinding and other co-operative phenomena

Manoj Gopalakrishnan ^(1,2), Kimberly Forsten-Williams ^{*(3)}, Eric Spiegel ⁽¹⁾,
Satheesh Angaiah ^(1,4), Matthew A. Nugent ⁽⁵⁾ and Uwe C. Täuber ⁽¹⁾

1 Department of Physics,
Virginia Polytechnic Institute and State University,
Blacksburg, VA 24061, USA.

2 [†]Max-Planck-Institut für Physik komplexer Systeme,
Nöthnitzer Straße 38,
01187 Dresden, Germany.

3 Department of Chemical Engineering,
Virginia Polytechnic Institute and State University,
Blacksburg, VA 24061, USA.

4 Department of Electrical and Computer Engineering,
Virginia Polytechnic Institute and State University,
Blacksburg, VA 24061, USA.

5 Department of Biochemistry,
Boston University School of Medicine,
Boston, MA 02118, USA.

Key words: Fibroblast growth factor-2 (FGF-2, bFGF), Monte Carlo simulations,
heparan sulfate proteoglycans, receptors, mean-field theory

Running Title: Enhanced Rebinding and Dissociation

^{*}corresponding author

[†] Present address

Abstract

Receptor-ligand binding is a critical first step in signal transduction and the duration of the interaction can impact signal generation. In mammalian cells, clustering of receptors may be facilitated by heterogeneous zones of lipids known as lipid rafts and *in vitro* experiments show that disruption of rafts significantly alters the dissociation of basic fibroblast growth factor (FGF-2) from its co-receptor heparan sulfate proteoglycans. We have addressed this question of altered dissociation in spatially inhomogeneous configurations via self-consistent mean-field theory and Monte Carlo simulations. We explore two possible mechanisms for the reduced dissociation found: (i) simple rebinding of dissociated ligands enhanced by clustering of receptor proteins due to spatial proximity, and (ii) rebinding facilitated by ‘internal diffusion’ and immediate binding by a neighboring receptor within the cluster. Monte Carlo simulations of the two raft models were performed where the simple rebinding (SR) model involves only mechanism (i) and the co-operative rebinding (CR) model incorporates both (i) and (ii). Our results show that the CR model is considerably more effective in reducing the effective dissociation rate as compared to SR model and compares well with experimental evidence. This work highlights the significance of internal diffusion within specialized zones for ligand retention.

1. Introduction

The cell membrane is composed of many different types of lipid species, and this heterogeneity leads to the possibility of organization of different species into distinct *domains* (Pike, 2004). Such domains are especially suited and designed for specialized functions such as signal transduction, nutrient adsorption and endocytosis. They have specific cellular machinery and physical features and are equipped with mechanisms for maintenance (addition and removal of specific molecules) for a certain period of time, during which the domains diffuse as single entities (Edidin, 2003). Lipid rafts, which are micro-domains rich in sphingolipids and cholesterol, represent one of the most interesting but insufficiently understood lipid domains (Munro, 2003). Various estimates are available for raft sizes, and diameters in the range 25-200 nm have been reported using various methods (Simons et al., 2004). A myriad of functions have been prescribed to lipid rafts with one possibility being a mediator of signal transduction for several growth factors, including fibroblast growth factor-2 (FGF-2) (Davy et al., 2000, Ridyard and Robbins, 2003, Chu et al., 2004).

Growth factors act as triggers for many cellular processes, and their action is mediated by transmembrane receptor proteins via ligand binding to the extracellular domain. For many receptors, signal transduction requires dimerization or clustering whereby two or more receptors either interact directly and are found in close proximity with each other, or are brought together following ligand binding. Certain growth factors bind to more than one receptor. For example, FGF-2 activates a cell surface receptor (CSR), but also binds to the heparan sulfate glycosaminoglycan chains of cell surface proteoglycans (HSPGs). HSPGs are a varied class of molecules and include the transmembrane syndecans, the glycosyl-phosphatidylinositol anchored glypicans, and extracellular proteoglycans such as perlecan (reviewed in Bernfield et al., 1999, Kramer and Yost 2003). The interaction of FGF-2 with HSPGs is of a lower affinity than the signaling receptor but has been shown to stabilize FGF-2-CSR binding and activation of CSR (Nugent and Edelman, 1992, Fannon and Nugent, 1996). Moreover, HSPG have recently been demonstrated to function directly as signaling receptors in response to FGF2 binding leading to the activation of protein kinase C alpha (Horowitz and Simons, 1998) and Erk1/2 (Chu et al., 2004).

There is recent evidence that cell surface HSPGs are not distributed uniformly, but are instead localized in lipid rafts (Wickstrom et al., 2003, Fuki et al., 2000, Chu et al., 2004). For example, syndecans have been shown to associate with detergent-insoluble membrane micro-domains (an operational definition of lipid rafts) (Couchman, 2003) and this association may be facilitated by FGF-2 binding and clustering (Tschachenko and Simons, 2002). This localization and clustering may have a dramatic effect on signaling via both localization and persistence. For example, FGF-2 binding to HSPG was decreased when cells were treated with the raft-disrupting agents methyl- β -cyclodextrin and filipin (Chu et al., 2004). Further, FGF-2 dissociation kinetics were significantly altered by these compounds (Fig. 1). Retention of FGF-2, even at long times, was significantly greater when lipid rafts were maintained however this effect was lost when soluble heparin, a competitor for HSPG binding, was included. These experiments

suggest that clustering of HSPG in lipid rafts effectively slows down dissociation by increasing the rebinding of released FGF-2. If this is indeed true, then the localization of binding sites to micro-domains on the cell surface could be a general mechanism employed by receptors to boost signal transduction.

The effect of clustering of receptors on the association rate of ligands has been addressed in several previous studies: the case of a cluster of two receptors was theoretically studied by Goldstein and coworkers (1983), while a single receptor cluster which also includes lateral diffusion of a bound ligand inside the cluster was investigated by Potanin et al. (1994). The emphasis in these studies was primarily on the reduction in the ligand flux due to the competition between receptors, an issue first addressed in the classic work of Berg and Purcell (1977), and the consequent reduction of the effective forward rate constant (although a non-monotonic change was predicted by Potanin et al. (1994) for large receptor clusters). The issue of rebinding in the context of receptor clusters has not been addressed before, to the best of our knowledge.

In this paper, we undertake a mathematical and computational study based on a lattice model to understand and quantify the role of receptor clustering in promoting the rebinding of dissociated ligands. Using a simplified view of the ligand-receptor interaction consisting of dissociation, diffusion, and diffusion-limited rebinding of ligands, we quantify the effect of raft size and distribution on the rebinding. In recent work, we obtained, for a spatially uniform distribution of receptors, the complete mathematical form of the non-exponential dissociation curve in the presence of the re-adsorption events under a self-consistent mean-field (SCM) theory (Gopalakrishnan et al., submitted). In the present paper, we extend this previous study on ligand rebinding to include receptor clusters. We identify two mechanisms whereby receptor clustering would slow down the effective dissociation of ligands: (i) by increasing the number of rebinding events over short distances and (ii) by enhancing the probability that a dissociated ligand will rebind to a neighboring free receptor, thus trapping it within the cluster for long periods of time. A model which incorporates only (i) is referred to as the ‘simple rebinding’ (SR) model in our paper. We present an approximate theoretical treatment of this model based on our earlier SCM theory, and demonstrate analytically that clustering of receptors leads to slower dissociation of ligands. A second variant that includes both mechanisms (i) and (ii) is referred to as the ‘co-operative rebinding’ (CR) model here. We have performed Monte Carlo simulations for both model variants, and conclude that co-operative binding activity is a necessary ingredient to produce dissociation curves comparable to experiments.

In the following two sections, we investigate these two model variants in detail. Sec. 2 deals with the SR model, where we present a modified version of SCM theory and discuss its predictions. In Sec. 3, we present and discuss the results of numerical simulations for both models. A brief summary and further discussion in Sec. 4 concludes this work.

2. Self-consistent mean-field (SCM) analysis of the simple rebinding (SR) model

2.1 SCM theory for a homogeneous distribution of receptors

In this section, we outline a self-consistent mean-field theory for ligand dissociation in the presence of rebinding events. For additional details, we refer the reader to Gopalakrishnan et al. (submitted). Let us consider a spatially homogeneous distribution of receptor molecules (binding sites) on a two-dimensional surface with mean area density P_0 . We define $p(t)$ to be the fraction of binding sites which are bound to ligands at time t , so that $p(0)$ is the fraction bound immediately following association. We denote the dissociation rate of ligands from the bound sites as β . The most general equation describing the time evolution of $p(t)$ within this framework is then

$$\frac{dp(t)}{dt} = -\beta p(t) + \gamma(t) \quad , \quad (1)$$

where $\gamma(t)$ represents the rate (probability per unit time) that a certain binding site will (re)absorb a ligand at time t . The basic stochastic event contributing to the rate $\gamma(t)$ is the dissociation of a ligand from a certain bound receptor during a given time interval $[\tau; \tau + d\tau]$, where $\tau < t$, and its subsequent adsorption at the reference site at time t . Our first simplification is to view the two-dimensional substrate surface as a (square) lattice of randomly mixed potential binding sites (depending on occupancy) and non-binding sites, with the former present on the surface at a density $\theta = P_0 \Delta^2 p_a$, where Δ is the lattice spacing and p_a is the absorption probability, which we equate to 1 for simplicity. The rebinding probability may then be expressed as

$$\gamma(t) = \beta \int_0^t d\tau p(\tau) \int dx dy \tilde{P}(x, y; t - \tau) \quad , \quad (2)$$

where

$$\tilde{P}(x, y; T) = \frac{1}{2\pi D T} \exp\left(-\frac{x^2 + y^2}{2 D T}\right) C_\theta(\Delta, T) \quad (3)$$

represents the probability of diffusion followed by adsorption of the ligand at the target site. In this expression, $C_\theta(\Delta; T)$ is the probability that a one-dimensional random walk starting at the point $z = \Delta$ at time $t = 0$ is adsorbed at $z = 0$ at $t = T$. Following a straightforward integration over the xy -plane, the rebinding probability becomes

$$\gamma(t) = \beta \int_0^t d\tau p(\tau) C_\theta(\Delta; t - \tau) \quad . \quad (4)$$

Equations 1 and 2 combined are formally solved using Laplace transforms, defined through $\tilde{p}(s) = \int_0^\infty p(t)e^{-st}dt$ and $\tilde{C}_\theta(s) = \int_0^\infty C_\theta(A; t)e^{-st}dt$. After re-writing Eq.4 in terms of these variables, and substituting in Eq.1, the solution for $\tilde{p}(s)$ is

$$\tilde{p}(s) = \frac{p(0)}{s + \beta[1 - \tilde{C}_\theta(s)]} . \quad (5)$$

$\tilde{C}_\theta(s)$ was previously computed (Gopalakrishnan et al., submitted) by exploiting the statistical independence of the returns of a random walk to its point of origin. It takes the form

$$\tilde{C}_\theta(s) = \frac{\theta \tilde{q}(s)}{1 - (1 - \theta) \tilde{q}(s)} , \quad (6)$$

where $\tilde{q}(s)$ is the Laplace transform of the first passage probability $q(A; t)$, defined as the probability that a random walk with diffusion coefficient D starting at $z=A$ at time $t=0$ first visits $z=0$ at time t . It can be shown that

$$\tilde{q}(s) = e^{-2\sqrt{\delta s}} , \quad (7)$$

where

$$\delta = \frac{A^2}{2D} \quad (8)$$

represents the microscopic diffusion time scale. We now assume that δ is sufficiently small (in comparison with $1/\beta$) so that the approximation $e^{-2\sqrt{\delta s}} \approx 1 - 2\sqrt{\delta s}$ can be used. With this simplification, we find that $1 - \tilde{C}_\theta(s) \approx (2/\theta)\sqrt{\delta s}$, and consequently, from Eq.5,

$$\tilde{p}(s) = \frac{p(0)}{s + \beta \frac{2}{\theta} \sqrt{\delta s}} . \quad (9)$$

This expression can be inverted explicitly (Erdelyi, 1954), leading to the final result

$$p(t) = p(0) e^{ct} \operatorname{erfc}(\sqrt{ct}) , \quad \text{where } c = \frac{4\beta^2 \delta}{\theta^2} \quad \text{and} \quad \operatorname{erfc}(z) = \frac{2}{\sqrt{\pi}} \int_z^\infty e^{-x^2} dx , \quad (10)$$

which characterizes a very slow dissociation process. The solution displays an expanded stretched exponential decay (Abramowitz and Stegun, 1970) at short times $t \ll 1/c$: $p(t) \approx p(0)[1 - (4\beta/\theta\sqrt{\pi})\sqrt{\delta t} + ..]$, whereas the very late time behavior becomes

algebraic: $p(t) \sim 1/\sqrt{t}$ when $t \gg 1/c$. We have thus shown that the rebinding events strongly modify the dissociation process, and the resulting effective temporal decay is far from exponential, even at relatively short times. The solution given in Eq.10 was found to fit quite nicely with data from surface plasmon resonance (SPR) experiments, as well as Monte Carlo simulations [Gopalakrishnan et al., submitted]. The self-consistent mean-field theory presented here shall be the basis of the analysis in the next section, where we extend it to study non-homogeneous distribution of receptors due to the presence of lipid rafts.

2.2 SCM theory for small rafts

In this section, we present an approximate theoretical treatment to study the effect of lipid rafts on ligand dissociation, based on the SCM theory outlined in the previous section. The presence of lipid rafts causes the receptor proteins to be trapped inside them with significantly reduced mobility for long periods of time. Within our simple description, we model these rafts as static clusters of binding sites, of radius R each. For simplicity, we also assume that the receptor proteins are static inside rafts. The most important assumption we invoke is that all the rebinding events may be classified into two:

- (i) Intra-raft rebinding, where a ligand dissociates and rebinds inside the same raft, and never leaves it during the process; and
- (ii) Inter-raft rebinding, where the origin and target site for the ligand are in different rafts.

For the rebinding events in the second category, we assume that the ligand effectively feels a homogeneous distribution of receptors on the surface, since it is likely to make several visits to the surface before finally binding to a receptor. Our last assumption is that there exists a characteristic length scale ξ which segregates rebinding events in category (i) from category (ii): all the dissociation-rebinding events separated by a distance less than ξ belong to (i), whereas all others belong to (ii). The length scale ξ is essentially of a phenomenological nature, and is not defined very precisely. For physical reasons, however, this length scale may be thought as being proportional to, and of the order of (although likely to be somewhat smaller than) the raft radius: i.e., $\xi \approx R$.

As in the previous section, we define $p_R(t)$ as the fraction of bound receptors. Its dynamics is described by the equation

$$dp_R(t)/dt = -\beta p_R(t) + \gamma_R(t), \quad (11)$$

where the new rebinding probability is written as the sum of intra-raft and inter-raft rebinding terms as explained above:

$$\gamma_R(t) = \beta \left[\int_0^t dt p_R(\tau) \int_0^\xi dr 2\pi r P(r; t-\tau) q(\Delta; t-\tau) + \int_0^t dt p_R(\tau) \int_\xi^\infty dr 2\pi r P(r; t-\tau) C_\theta(\Delta; t-\tau) \right]. \quad (12)$$

In this equation, $q(\Delta; t)$ is the first passage probability defined in the last section and $P(r; T) = (2\pi DT)^{-1} \exp(-r^2/2DT)$ is the probability that a ligand covers a distance R in the

horizontal plane in a time T , and D denotes the ligand diffusion coefficient. After completing the straightforward spatial integration in Eq.12, we arrive at

$$\gamma_R(t) = \gamma(t) + \beta \left[\int_0^t d\tau p(\tau) [1 - \exp(-\xi^2 / 2D(t-\tau))] [q(\mathcal{A}; t-\tau) - C_\theta(\mathcal{A}; t-\tau)] \right] , \quad (13)$$

where $\gamma(t)$ represents the ‘average’ rebinding probability in the absence of rafts given by Eq.4. We have further assumed in Eq.13 that the raft packing density of receptor proteins is at its maximum, i.e., $\theta = 1$ inside rafts. [In general, the rafts may be assumed to have a higher coverage fraction $\theta' > \theta$, in which case $q(\mathcal{A}; t) \equiv \tilde{C}_1(\mathcal{A}; t)$ is to be replaced by $\tilde{C}_{\theta'}(\mathcal{A}; t)$.] We now define the quantities

$$G_1(t) = [q(\mathcal{A}; t-\tau) - C_\theta(\mathcal{A}; t-\tau)] \quad \text{and} \quad G_2(t) = e^{-\frac{\xi^2}{2Dt}} G_1(t) , \quad (14)$$

along with their Laplace transforms $\tilde{G}_1(s)$ and $\tilde{G}_2(s)$, as well as the Laplace transform $\tilde{p}_R(s)$ of the rebinding probability as in the previous section. The modified expression for $\tilde{p}_R(s)$ after substituting these quantities, reads

$$\tilde{p}_R(s) = \frac{p(0)}{s + \beta(1 - \tilde{C}_\theta(s)) - \beta\Sigma(\xi; s)} , \quad (15)$$

where

$$\Sigma(\xi; s) = \tilde{G}_1(s) - \tilde{G}_2(s) \quad (16)$$

denotes the correction to the homogeneous expression in Eq.9 due to the presence of rafts. From Eqs. 6 and 14, we find that

$$\tilde{G}_1(s) \equiv g(\delta; s) = \frac{(1-\theta)\tilde{q}(s)[1-\tilde{q}(s)]}{1-(1-\theta)\tilde{q}(s)} . \quad (17)$$

We now consider the limit where the microscopic time scale $\delta \rightarrow 0$ (i.e., we are interested in time scales $t \gg \delta$), in which case Eq.17 may be approximated to

$$\tilde{G}_1(s) \equiv g(\delta; s) \approx \frac{2(1-\theta)\sqrt{\delta s}}{\theta + 2(1-\theta)\sqrt{\delta s}} e^{-2\sqrt{\delta s}} . \quad (18)$$

after using Eq.7. Next, in order to compute $\tilde{G}_2(s)$, we first invert this relation (Erdelyi, 1954) and find $G_1(t)$, which turns out to have the form $G_1(t) \propto (\mathcal{A} / t\sqrt{Dt}) e^{-\frac{\delta}{t}}$ for $t \gg \delta$.

From the second part of Eq.14, we subsequently find that, when $\xi \gg \Delta$,
 $\tilde{G}_2(s) = (\Delta/\xi)g(\delta'; s)$, where

$$\delta' = \xi^2/2D , \quad (19)$$

represents a second characteristic time scale in the problem and the function $g(\delta'; s)$ is defined by Eq.18. After substitution in Eq.16, we obtain (for small δ and δ')

$$\Sigma(\xi; s) \approx \frac{2(1-\theta)}{\theta} \sqrt{\delta s} \left[e^{-2\sqrt{\delta s}} - e^{-2\sqrt{\delta' s}} \right] , \quad (20)$$

which may be substituted into Eq.15. From Eqs.8 and 19, this correction term vanishes as $\xi \rightarrow \Delta$, as it should. We now specialize to the case of very small rafts, where this term is non-zero, but small, i.e., when $\xi/\Delta \sim O(1)$. We may then expand Eq.15 as a perturbation series in Σ . After keeping only the first term for simplicity, this series has the form

$$\tilde{p}_R(s) = \frac{p(0)}{s + 2\frac{\beta}{\theta}\sqrt{\delta s}} + \frac{p(0)\beta\Sigma(\xi; s)}{\left[s + 2\frac{\beta}{\theta}\sqrt{\delta s}\right]^2} + O(\Sigma^2) . \quad (21)$$

When the time scales δ and δ' are small (compared to $1/\beta$), we may further simplify Eq.20 to obtain $\Sigma(\xi; s) \approx 4\delta s(\theta^{-1} - 1)(\xi/\Delta - 1)$. After substituting this expression into Eq.21, the resulting expression can be inverted, and the leading behavior in the large time ($t \gg \delta', \delta$) limit is given by

$$p_R(t) \equiv p(t) + \hat{p}_R(t) , \quad (22)$$

where $p_R(t)$ is defined as the bound fraction of ligands in the presence of rafts, $p(t)$ is the fraction for the homogeneous case (defined by Eq.10), and $\hat{p}_R(t)$ is the difference between these two fractions. Our explicit result for this quantity (after inverting Eq.21) eventually becomes (Erdelyi 1954)

$$\hat{p}_R(t) \approx 4\beta\delta(\theta^{-1} - 1) \left(\frac{\xi - \Delta}{\Delta} \right) \left[1 + \left(8(\beta/\theta)^2 \delta t - 1 \right) e^{ct} \operatorname{erfc}(\sqrt{ct}) - (\beta/\theta) \sqrt{\delta t/\pi} \right] + O \left[\left(\frac{\xi - \Delta}{\Delta} \right)^2 \right] . \quad (23)$$

Several important observations can already be inferred from this expression. The correction term vanishes as $\theta \rightarrow 1$ (i.e., organizing receptor proteins in rafts has negligible effect on dissociation when the surface coverage is high), and gains in significance as $\theta \rightarrow 0$. We also note that this term is inversely proportional to the diffusion coefficient D from Eq.8: when the diffusion coefficient is high, the ligands are able to travel across a raft faster, effectively averaging over the spatial distribution of

receptors; the dissociation curve is then only sensitive to the average number of receptor proteins and not to their spatial organization.

For large times $t \gg \delta$, we may use the asymptotic expansion of the complementary error function (Abramowitz and Stegun, 1970) in Eq.23. The leading term turns out to be a constant, i.e.

$$\hat{p}_R(t) \approx \frac{4\beta\delta(1-\theta)}{\theta} \frac{(\xi - \Delta)}{\Delta} \left[1 + O\left(t^{-3/2}\right) \right] ; \quad t \gg \delta , \quad (24)$$

so that, over intermediate time scales $\delta \ll t \ll 1/c$, the effect of clustering of receptor sites is to simply shift the dissociation curve upwards by a constant, proportional to the size of the rafts. This is a very nice result, and we shall see in the next section that this upward shift of the dissociation curve is indeed observed in numerical simulations (which in fact provides an *a posteriori* justification for our assumptions in this section).

3. Monte Carlo simulations

3.1 Lattice model of ligand-receptor binding

In order to perform numerical simulations of the dissociation-rebinding process, we construct a lattice model of a cell surface as follows. The cell surface is imagined as a two-dimensional square lattice of dimensions $L \times L$ where a fraction θ of the lattice sites are occupied by receptor proteins, i.e., they serve as potential ligand binding sites. The remainder of the sites are non-binding and the ligands are ‘reflected’ from these sites upon contact by diffusion. In a typical simulation, we have N rafts on the surface, distributed randomly each with ‘radius’ $\tilde{R} = R/\Delta$ (where Δ is the lattice spacing, as discussed above). The radius \tilde{R} was generally chosen such that a maximum number of the total $L^2\theta$ receptor sites could be included inside the rafts and the remaining binding sites were distributed randomly on the surface. The ligands are modeled as random walkers diffusing about in the semi-infinite three-dimensional volume, of which the cell surface forms the boundary. Ligands are either present in the solution or bound to the receptors on the surface. Fig. 2 shows two typical raft configurations used in our simulations.

The ligand diffusion is governed by periodic boundary conditions on the four borders of the lattice so that a ligand that exits at one boundary re-enters from the opposite side. The direction perpendicular to the plane of the lattice shall be referred to as the z-axis, and the surface itself is located at $z=0$. The ligand diffusion in the z-direction is not bounded. We also neglect surface diffusion of the receptor proteins, irrespective of them being clustered or isolated, and treat them as static objects throughout this paper (see, however, the discussion at the end of this section). The lattice dimension is fixed at $L = 100$ for all the simulations reported here.

At the beginning of the dynamics, a fraction, $p(0)$, of all the binding sites are bound to a ligand each, i.e., the total number of ligands in the system is $N = L^2\theta p(0)$, and is

conserved throughout the simulation. There are three main dynamical processes in the simulation: (i) Dissociation of a ligand from a bound receptor takes place with probability $\tilde{\beta}$ per time step. This move updates the position of the ligand from $z=0$ to $z=2$, in units of the lattice spacing (we use $z=2$ instead of $z=1$ in order to prevent immediate rebinding to the same receptor). (ii) Diffusion of the released ligands in solution: A free ligand moves a distance equal to one lattice spacing in one of the six directions with probability $\tilde{D}=1/6$ per time step. (iii) Re-adsorption of free ligands to free receptors: A free ligand at $z=1$ is absorbed by a free receptor below it, if there is one, with probability which we set to unity in all the simulations reported here (i.e., the ligand-receptor binding is assumed to be entirely diffusion-limited). The lattice spacing and the diffusion time step represent the fundamental microscopic length and time scales in the problem, and their precise meaning is discussed below.

The smallest microscopic length scale at the level of receptor organization on the cell surface is simply the typical receptor size $\sim 5\text{nm}$, and we use this value as our choice for \mathcal{A} . (We note that the mean free path of a free ligand in solution would constitute a more microscopic estimate, and this was in fact chosen in Gopalakrishnan *et al.* (submitted)). Our choice here is based primarily on computational efficiency. Also, since our interest here is centered mainly at studying the effects of receptor organization over length scales of $\sim 100\text{nm}$ (see the discussion below), we believe that the precise choice of the microscopic length scale should not have a significant effect on our results. With this choice of \mathcal{A} , the microscopic time scale is estimated to be $\delta \approx 10^{-6}\text{s}$ (after using an estimate of $D \approx 10^{-6}\text{cm}^2\text{s}^{-1}$).

For ‘typical’ dissociation rates (for example, β for FGF2-HSPG coupling has been measured as $\sim 0.1\text{ min}^{-1}$ (Nugent and Edelman, 1992)), the dissociation time scale ($\sim 1/\beta$) is of the order of a few minutes, which far exceeds the diffusion time scale. Thus, the natural choice of the unit of time in the simulation is the diffusion time scale. In the simulations, we choose a dissociation rate per unit time step, $\tilde{\beta} \approx \beta\delta t$, where $\delta t = \mathcal{A}^2/6D = \delta/3$ is the diffusion time scale. The total number of Monte Carlo steps in a single simulation run is $N=100/\tilde{\beta}$ (equivalent to about 100 times the dissociation time scale). To limit computational time, therefore, we fixed $\tilde{\beta} = 10^{-5}$ in all the simulations. The resulting dissociation curve is then averaged over 20 different starting configurations.

We now proceed to the distribution of receptors on the cell surface and the selection of the raft sizes we used in the simulations. Various experiments have predicted different values for raft sizes. The diameter of rafts has been estimated to be as low as 4 nm, or as high as 700 nm (reviewed in Anderson and Jacobsen, 2002), and seems to depend on the cell type and the measurement method used. Several independent measurements, however, seems to suggest a diameter of 40-70 nm (Simons *et al.*, 2004). In most of the simulations reported here, we have chosen the raft radius to be $\tilde{R} = 8.0$, which corresponds to a diameter of nearly 80 nm. In the square lattice we used in our

simulations, such a raft contains about 200 lattice sites. There have been suggestions that a raft is likely to contain no more than $\sim 50\text{-}70$ proteins, depending on the packing density (Pralle et al., 2000). However, in all the simulations reported here, we have chosen the maximum packing density for proteins inside a raft (i.e., all the sites inside the raft are potential binding sites).

As already mentioned in the introduction, we have studied two models of lipid rafts in this paper. In the first model, which we henceforth refer to as the simple rebinding (SR) model, the receptor proteins inside a cluster are assumed to be sufficiently distant from each other so that co-operative interactions between receptors are essentially absent. In this model, receptor clustering affects rebinding only by increasing the probability of recapture during the first few returns of a dissociated ligand to the surface. This model may also be viewed as the ‘pure diffusion limit’ of the raft model (since no other mechanism is involved in rebinding). From another perspective, if the receptor proteins inside a raft are sufficiently far from each other, any direct interaction between them will be presumably non-existent or weak. In this sense, the SR model may also be seen as the ‘dilute limit’ of rafts.

In our second model variant, which we shall refer to as the co-operative rebinding (CR) model, we include explicit coupling between receptors inside rafts. That is, a ligand, following dissociation from a bound receptor, will attempt to immediately bind to one of the neighboring unbound receptors (if one is available) before diffusing in solution. Clearly, the effects of receptor clustering will be much more pronounced in this variant. This model explicitly incorporates co-operative effects between receptors, whereas such effects are only implicit (namely, through the reactions being diffusion-controlled) in the SR model.

3.2 Numerical results for the SR model

In this section, we first present and discuss the numerical results for the simple rebinding model. In Fig. 3 (A), we plot the dissociation data for $\theta=0.1$ for three cases of receptor distributions, namely: (a) homogeneous, (b) 5 rafts with radius $\tilde{R}=8.0$ each, and (c) a single raft with radius $\tilde{R}=18.0$. We observe that the clustering of binding sites leads to measurably slower dissociation as compared to the homogeneous case. We also observe that the slowing effect is monotonic in raft size: the larger the raft, the slower is the dissociation. In Fig. 3 (B), we show the corresponding results for a higher surface coverage, $\theta=0.5$. In this case, the difference between the curves has significantly diminished, and is in fact almost non-existent. This result is physically reasonable (when too many sites are available for binding, clustering is bound to become insignificant), and also agrees with the conclusions from the self-consistent mean-field (SCM) theory presented in Sec. 2.

In order to quantify the effect of rafts in reducing the effective dissociation, we studied the difference between the dissociation curves in the presence and absence of rafts, defined as $\hat{p}_R(t)$ in Eq.22, for $\tilde{R}=8.0$ and $\tilde{R}=18.0$. The result for $\theta=0.1$ is plotted in Fig. 4 as a function of time. We observe that the difference initially rises, and then

appears to fluctuate around a stationary value. This observation also agrees with the prediction of Eq.24 obtained from the SCM approximation.

The theoretical prediction for the ‘asymptotic’ difference may be calculated from Eq.24 using the approximate substitution $\zeta = R$. The dissociation rate equivalent to the number used in the simulations is given through the relation $\beta\delta = 3\tilde{\beta} = 3 \times 10^{-5}$. For $\tilde{R} = 8.0$ and 18.0, the differences turn out to be $\hat{p}_R^\infty \approx 0.0075$ and 0.01836, respectively. The corresponding numerical values of $\hat{p}_R(t)$, averaged in the time interval $t = 60/\tilde{\beta}$ to $t = 100/\tilde{\beta}$ are 0.0253 (± 0.0046) and 0.0407 (± 0.0048). The agreement with the theoretical prediction is good, although not quantitatively accurate. This, however, should not be viewed as a serious drawback of the model. Recall that the SCM theory presented in Sec. 2.2 is based on several simplifying assumptions. In any case, Eq.24 itself is the result of merely a perturbative analysis, and is valid only for sufficiently small raft sizes.

In order to gain further insight into the mechanisms by which rafts can enhance ligand rebinding, we monitored the probability distribution of the rebinding distance. This quantity is denoted by $Q(r)$, and is defined as the probability that a ligand which dissociates from one site in the lattice will rebind at a site a distance r from the starting point, averaged over the time of dissociation and the time interval of transit. This quantity is, therefore, only sensitive to the organization of the binding sites on the lattice.

In Fig. 5, we show the distribution $Q(r)$ plotted against the distance r on a logarithmic scale, for three situations: (a) homogeneous distribution of receptors, (b) 3 rafts with radius $\tilde{R} = 8.0$ and (c) 5 rafts with radius $R = 8.0$. The surface coverage is kept constant at $\theta = 0.1$ in all the cases. This means that, for case (b), in particular, a sizeable fraction of receptors were outside the rafts and were distributed at random. For case (c), however, more than 97% of the receptors were located inside the rafts. The following observations may be made from Fig. 5: (i) For a homogeneous distribution, there is only a weak dependence on the distance, and the function $Q(r)$ is essentially flat before dropping abruptly at the system size limit (here, at about $r \sim 60$). (ii) For $N=5$, $\tilde{R}=8.0$, we can clearly identify two regimes: Many rebinding events occur at short distances, and $Q(r)$ decreases monotonically from its maximum at $r=0$ until a cut-off length scale $r^* \approx 16$ is reached. After this, $Q(r)$ rises again until it drops off abruptly at the system-size limit. (iii) For the case of $N=3$, $\tilde{R}=8.0$ shows the transition between these different behaviors.

The physical picture provided by this analysis may be summarized as follows. At short distances, many consecutive rebinding events take place inside the rafts since the adsorption surface there is almost at saturation ($\theta = 1$). This is represented in the first regime mentioned above. The cut-off length scale for this regime roughly matches the raft diameter, in agreement with the assumptions made in Sec. 2.2 for the SCM theory. At length scales far beyond the raft diameter, inter-raft rebinding events gain prominence, but the ligands in this case ‘sense’ only the average receptor density since the effects of

spatial organization are effectively wiped out. We also observe that the short-distance rebinding events become enhanced for stronger clustering (note the upward shift of $Q(0)$ as the number of rafts increases).

In order to further verify the validity of these arguments, we also simulated a system of 5 rafts of radius $\tilde{R}=8.0$, where the rafts are spatially distributed in a periodic fashion, as displayed in Fig. 6 (A). The rebinding distance distribution obtained from this model can then be compared to the $N=5$, $\tilde{R}=8.0$ case discussed above (where the raft distribution was homogeneous), see Fig. 6 (B). We observe that a second, less pronounced peak appears in the distribution corresponding to rebinding events taking place between *two* neighboring rafts, which are at a fixed distance from each other. The dissociation curve, however, was not affected by this change (data not shown).

To summarize, the simple rebinding model of rafts predicts marked enhancement of rebinding and the consequent slowing of dissociation of ligands. We have also successfully quantified this change within the self-consistent mean field formalism developed earlier for a homogeneous receptor distribution, adapted to include receptor clusters. However, the reduction in dissociation rates observed in this model is far lower than what has been observed in *in vitro* cell experiments, where the dissociation curve was almost flat when the rafts were present and dropped substantially when rafts were disrupted by chemical treatment (Fig 1). Our conclusion is, therefore, that enhanced rebinding alone is insufficient to account for the experimental observations, and further mechanisms need to be explored. For this purpose, we introduce the co-operative rebinding model to be discussed in the next section.

3.3 The co-operative rebinding (CR) model

In the co-operative rebinding model, we assume that a ligand, once it dissociates from a bound receptor, would preferentially attempt to bind to a free receptor in its immediate vicinity, before becoming free. In this model, therefore, a bound ligand effectively performs ‘internal diffusion’ inside a raft through this dissociation-cum-hopping process (provided there are a sufficient number of free receptors) before it finally dissociates from the raft, which will happen most likely after it has reached the edge. A similar model was used in Potanin *et al.* (1994) to study the effect of receptor clustering on the association process.

The effect of this internal diffusion on the dissociation rate may be quantified through the following simple argument. Given that a ligand will hop from one receptor to the next over a time scale $\tau \sim \beta^{-1}$, its effective diffusion coefficient inside the raft is simply $D_R \sim \Delta^2 \beta$. The time taken for the ligand to traverse the raft is then $T \approx R^2 / D_R \sim (R/\Delta)^2 \beta^{-1}$, which may also be viewed as the typical time interval between two dissociation events. The effective dissociation rate is thus reduced to

$$\beta_R \approx \beta \left(\frac{\Delta}{R} \right)^2. \quad (25)$$

When $R/\Delta \sim 10$ (a typical value), for example, the effective dissociation rate is reduced by a factor of 100. The internal hopping mechanism in this model is, therefore, very effective in slowing down the average dissociation. Fig. 7 shows the simulation results of the dissociation curve for the CR model, for surface coverages $\theta = 0.1$ (A) and $\theta = 0.5$ (B). In Fig. 7 (A), we present the results for a homogeneous distribution of receptors, as well as the cases $N=3$, $\tilde{R} = 8.0$, and $N=5$, $\tilde{R} = 18.0$. We observe a dramatic effect of clustering on the effective dissociation, at a level comparable to the experimental observations (Fig. 1).

In Fig. 7 (B), we see that when the coverage is as high as $\theta = 0.5$, dissociation is very slow and almost non-existent even for a homogeneous receptor distribution. This could possibly be the consequence of a percolation effect. The percolation threshold for site percolation in a two-dimensional square lattice is $p_c \approx 0.4$ (Stauffer, 1975). Thus, when the fraction of binding sites is greater than 0.4, in an infinitely extended system a connected cluster of binding sites forms with probability one that spans the lattice. This is essentially what is observed for a random distribution of receptors. A ligand initially bound to a receptor that belongs to this ‘infinite’ cluster is likely to diffuse inside this cluster almost forever, and this produces the extremely slow dissociation curves apparent in Fig. 7 (B).

The relevance of the CR model to the FGF-2-HSPG system may be understood from the structure of the HSPG protein. Glycosaminoglycan sidechains can extend over 60 nm in length (Nomura et al., 2003), although the core protein may not be more than 10 nm in diameter. It is therefore conceivable that the chains from one molecule overlap with those from another, especially in the confining geometry provided by a lipid raft. Hopping of a ligand from one molecule to another is therefore possible, and this would lead to the effective confinement of the FGF-2 molecule inside a raft for long periods of time (compared to the time scale of the intrinsic dissociation rate).

4. Discussion

It is generally understood that lipid rafts are capable of confining several kinds of large proteins inside them for time scales up to several minutes (Edidin, 2003). Heparan sulfate proteoglycans (HSPG) are among the proteins shown to localize to lipid rafts, and they are also co-receptors for the basic fibroblast growth factor (FGF-2). We therefore sought to determine theoretically whether the confinement and clustering of HSPG inside lipid rafts would affect binding of FGF-2, either via promoting rebinding of dissociated ligands or via reduced dissociation through some co-operative interactions between HSPG in close proximity to each other. Experimental studies indicate that lipid rafts play a significant role in controlling the dissociation of FGF-2 from HSPG, but the mechanism behind this effect was unclear (Fig. 1, (Chu et al., 2004)).

In this paper, we explored two possible mechanisms by which lipid rafts might slow down ligand dissociation via trapping their receptor proteins: enhanced rebinding and internal diffusion. We constructed mathematical and computational models of rafts incorporating one or both of these mechanisms, and studied their relative importance. Our

conclusion is that enhanced rebinding alone is insufficient to explain the experimental observations, and that a model incorporating dissociation-cum-internal diffusion of ligands inside rafts could better account for the experimental data. It should be noted that our model does not include either internalization or synthesis of new receptors, processes of importance for comparison with studies at 37°C rather than 4°C. We also focus only on a single class of binding sites and do not include secondary receptors or receptor dimerization or coupling. Finally, the model as presented does not allow for receptor diffusion in and out of lipid rafts or the dissolution or formation of new rafts. These caveats are currently being examined for model extensions.

Our self-consistent mean-field theory, originally developed with the goal to investigate ligand rebinding for a uniform distribution of receptors, has served as a valuable tool in this present study of receptor clusters as well. With some simple modifications and a few assumptions, we were able to predict mathematically (albeit in a perturbative manner) by how much dissociation would be altered through clustering of receptors. The predictions of the model were found to compare favorably with both experiments and numerical simulations.

How stable is the association of a protein to the raft? Single-particle tracking experiments have shown that the diffusion of a raft-associated protein is unchanged over times scales of up to 10 min, indicating that the proteins remained with the raft during this period (Pralle *et al.*, 2000). However, since the dissociation measurements typically extend considerably longer (on the order of hours), the possibility of the proteoglycans exiting the raft during this period cannot be ruled out. It would be interesting to see, in a future study, if such dissociation events could have any impact on the rebinding process by making the surface coverage factor time dependent inside rafts. Other relevant issues that would be worthwhile investigating in this context include the effects of raft diffusion and their stability.

We thank H.J. Hilhorst, Y. Kafri, R. Kree, D. Lubensky, B. Schmittmann, and M. Zapotocky for fruitful discussions. Financial support from the National Science Foundation [awards NSF-DMR 0089451 (MG), NSF-9875626 (KFW), and NSF-DMR 0308548 (UCT)], National Institutes of Health [NIH-HL56200 (MAN)], and from the Bank of America Jeffress Memorial Trust [Grant no. J-594 (UCT)] is gratefully acknowledged.

References

Abramowitz, M., and I. A. Stegun. 1970. *Handbook of Mathematical Functions*. Dover, New York.

Anderson, R. G. W, and K. Jacobson. 2002. A role for lipid shells in targeting proteins to caveolae, rafts and other lipid domains. *Science*. 296: 1821-1825

Berg, H. C., and E. M. Purcell. 1977. Physics of chemoreception. *Biophys. J.* 20: 193-219

Bernfield M, M. Gotte, P. W. Park, O. Reizes and M. L. Fitzgerald .1999. Functions of cell surface heparan sulfate proteoglycans. *Annu. Rev. Biochem.* 68: 729-77

Chu, C. L, J. A. Buczak-Thomas, and M. A. Nugent. 2004. Heparan sulfate proteoglycans modulate fibroblast growth factor-2 binding through a lipid raft mediated mechanism. *Biochem. J.* 379: 331-341

Couchman, J. R. 2003. Syndecans: proteoglycan regulators of cell-surface microdomains? *Nat. Rev. Mol. Cell. Biol.* 4: 926-37

Davy, A., C. Feuerstein and S. M. Robbins. 2000. Signaling within a caveolae-like membrane microdomain in human neuroblastoma cells in response to fibroblast growth factor. *J. Neurochem.* 74: 676-83

Edidin, M. 2003. The state of lipid rafts: from model membranes to cells. *Annu. Rev. Biophys. Biomol. Struct.* 32: 257-283

Erdelyi, A (ed.). 1954. *Tables of Integral Transforms*. McGraw Hill, New York.

Fannon, M., and M.A. Nugent. 1996 Basic fibroblast growth factor binds its receptors, is internalized, and stimulates DNA synthesis in Balb/c3T3 cells in the absence of heparan sulfate. *J. Biol. Chem.* 271: 17949-17956

Fuki, I. V., M. E. Meyer and K. J. Williams. 2000. Transmembrane and cytoplasmic domains of syndecan mediate a multi-step endocytic pathway involving detergent-insoluble membrane rafts. *Biochem. J.* 351 (Pt 2): 607-612

Goldstein, B., and F. W. Wiegel. 1983. The effect of receptor clustering on diffusion-limited forward rate constants. *Biophys. J.* 43: 121-125

Gopalakrishnan, M., K. Forsten-Williams, T. R. Cassino, L. Padro, T. E. Ryan, and U. C. Täuber. 2004. Ligand rebinding: self-consistent mean-field theory and numerical simulations applied to SPR studies. Submitted to *Biophys. J.*

Horowitz, A. and M. Simons. 1998. Phosphorylation of the cytoplasmic tail of syndecan-4 regulates activation of protein kinase C alpha. *J. Biol. Chem.* 273:25548-25551

Kramer, K. L, and H. J. Yost. 2003. Heparan sulfate core proteins in cell-cell signaling. *Annu. Rev. Genet.* 37: 461-484

Munro, S. 2003. Lipid rafts: elusive or illusive? *Cell* 115: 377-388

Nomura Y., Y. Abe, Y. Ishii, M. Watanabe, M. Kobayashi, A. Hattori and M. Tsujimoto. 2003. Structural changes in the glycosaminoglycan chain of rat skin decorin with growth. *J. Dermatol.* 30: 655-664

Nugent, M. A., and E. R. Edelman. 1992. Kinetics of basic fibroblast growth factor binding to its receptor and sulfate proteoglycan: A mechanism for co-operativity. *Biochemistry* 31: 8876-8883

Pike, L. J. 2004. Lipid rafts: heterogeneity on the high seas. *Biochem. J.* 378 (Pt 2): 281-292

Potanin, A. A., V. V. Verkhusha, O. S. Belokoneva and F. W. Wiegel. 1994. Kinetics of ligand binding to a cluster of membrane-associated receptors. *Eur. Biophys. J.* 23: 197-205

Pralle, A., P. Keller, E.-L. Florin, K. Simons and J. K. H. Hörber. 2000. Sphingolipid-cholesterol rafts diffuse as small entities in the plasma membrane of mammalian cells. *J. Cell. Biol.* 148: 997-1007

Ridyard, M.S., and S.M. Robbins. 2003. Fibroblast growth factor-2-induced signaling through lipid raft-associated fibroblast growth factor receptor substrate 2 (FRS2). *J. Biol. Chem.* 278:13803-13809

Simons, K., and W. L. C. Vaz. 2004. Model systems, lipid rafts and cell membranes. *Annu. Rev. Biophys. Biomol. Struct.* 33: 269-295

Stauffer, D. 1975. *Introduction to Percolation Theory*. Taylor and Francis, London

Tkachenko, E., and M. Simons. 2002. Clustering induces redistribution of syndecan-4 core protein into raft membrane domains. *J. Biol. Chem.* 277: 19946-19951

Wickstrom S. A., K. Alitalo and J. Keski-Oja 2003. Endostatin associates with lipid rafts and induces reorganization of the actin cytoskeleton via down-regulation of RhoA activity. *J. Biol. Chem.* 278: 37895-37901

Figure Legends

FIG 1. (A) Effect of HSPG reduction on FGF-2 Dissociation: Bovine aortic smooth muscle cells (Coriell Cell Repositories (Camden, NJ)) were treated with (■) or without (□) heparinase III (0.1 U/ml, 1h, 37°C) (gift from Dr. E. Denholm from Biomarin Technologies (Montreal, Canada)), washed, and incubated with ^{125}I -FGF-2 (0.28 nM) for 2.5h at 4°C. Cells were washed and switched to binding buffer without FGF at t=0 and HSPG binding quantified using a high salt wash at the indicated time as described previously (Fannon and Nugent, 1996). Mean values of triplicate samples \pm SEM are shown (B) Effect of the Lipid Raft Disrupting Agent M β CD and heparin on dissociation from HSPGs. Dissociation experiment was performed as described in A but cells were treated with M β CD (0 or 10 mM) for 2h at 37°C prior to cooling to 4°C. Dissociation was done in binding buffer with or without heparin (100 $\mu\text{g}/\text{ml}$) to assist in preventing rebinding. Mean values of triplicate samples \pm SEM are shown (data replotted from Chu et al., 2004).

FIG 2. Two typical raft configurations used in simulations: (A) $N=5$ and $\tilde{R}=8.0$, and (B) $N=20$ and $\tilde{R}=8.0$. The surface coverage is $\theta = 0.1$ in (A) and $\theta = 0.5$ in (B).

FIG 3. The (normalized) numerical dissociation data for the simple rebinding (SR) model plotted against the scaled time $T = \tilde{\beta}t$ (t is measured in number of Monte Carlo steps): (A) for $\theta = 0.1$, and (B) for $\theta = 0.5$.

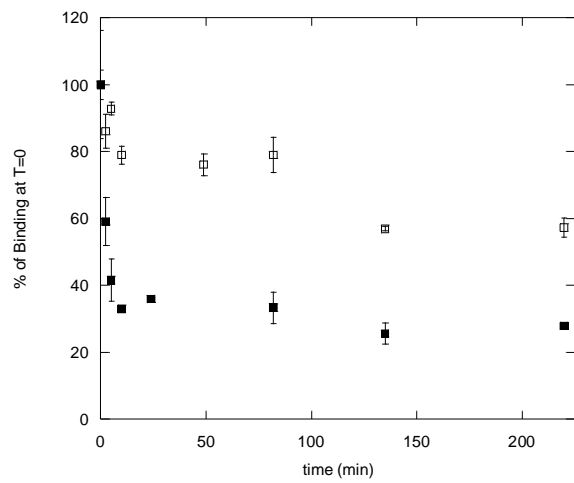
FIG 4. The difference between the (normalized) numerical dissociation data of clustered receptors (i.e., with rafts present) and a homogeneous distribution of receptor proteins in the SR model, plotted against the scaled time. The upper curve corresponds to $N = 1, \tilde{R} = 18.0$ and the lower curve to $N = 5, \tilde{R} = 8.0$. The straight lines show the mean values of these differences, averaged between T=60 and T=100.

FIG 5. The probability distribution $Q(r)$ of rebinding distance (as defined in Sec. 3.2) in the SR model plotted against the distance r , for the case $\theta = 0.1$. The distribution is nearly flat up to the system size cut-off (at $r \sim 60$) for the homogeneous distribution. Two distinct regimes are observed when rafts are present, corresponding to intra-raft and inter-raft rebinding events (see the discussion in the text).

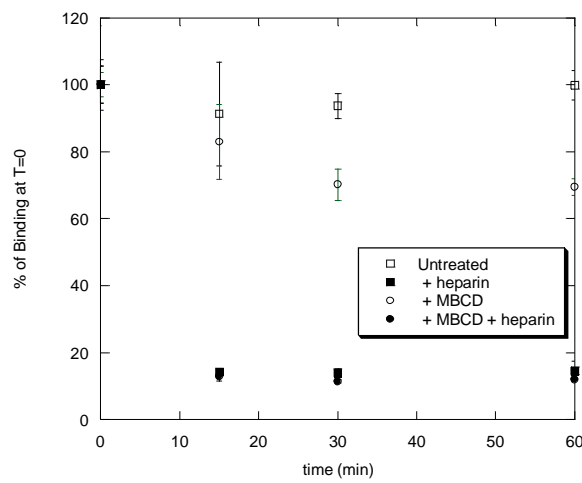
FIG 6. (A) A periodic distribution of 5 rafts, with radius $\tilde{R} = 8.0$, and (B) the corresponding probability distribution $Q(r)$ for the rebinding distance. Unlike in the data obtained for the case of randomly distributed rafts, also depicted in Fig. 5, three distinct regimes are observed for periodic raft arrays. The additional peak in the periodic arrangement data at intermediate distances corresponds to rebinding events taking place between neighboring rafts.

FIG 7. The numerical dissociation data for the CR model for coverages (A) $\theta = 0.1$, and (B) $\theta = 0.5$. In both cases, the bound fraction of ligands is plotted against the scaled time.

Figures

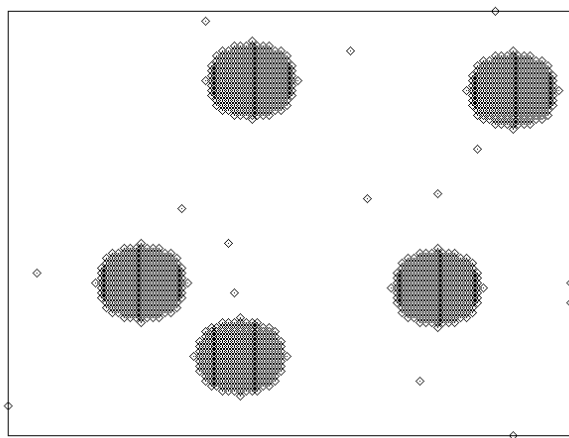


(A)

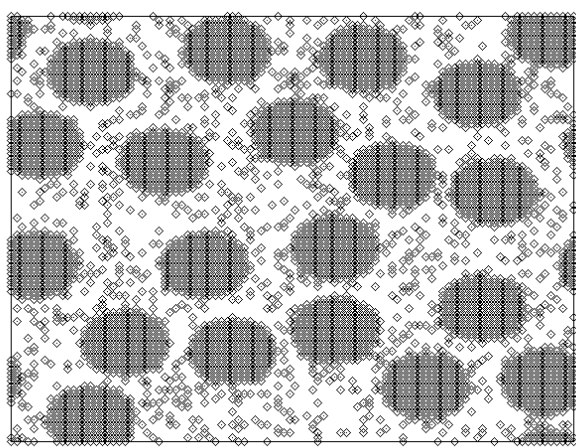


(B)

Fig 1

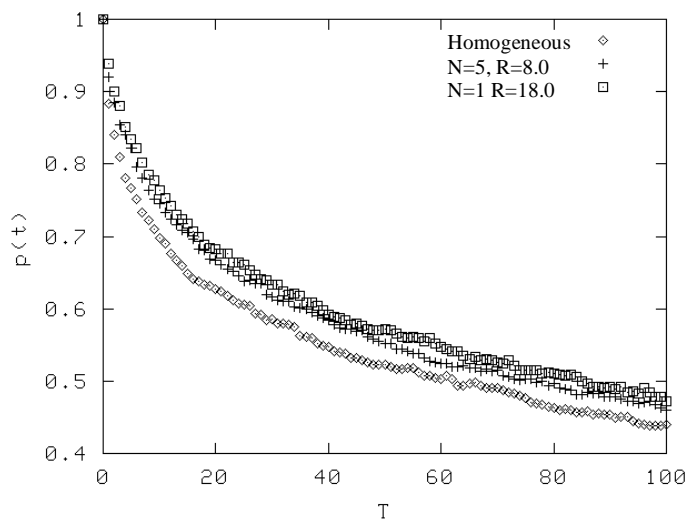


(A)

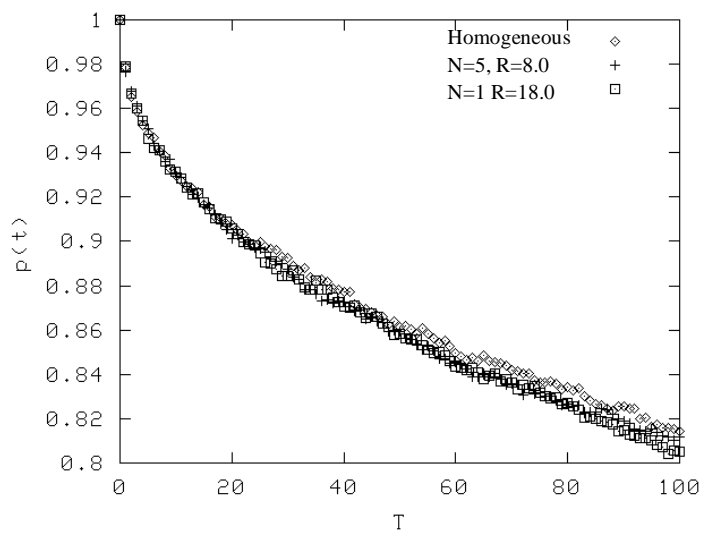


(B)

Fig 2



(A)



(B)

Fig 3

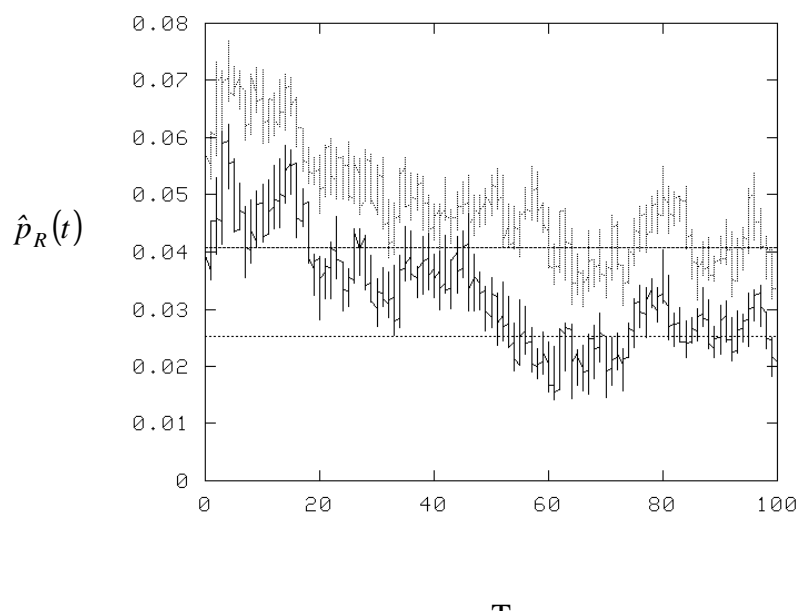


Fig 4

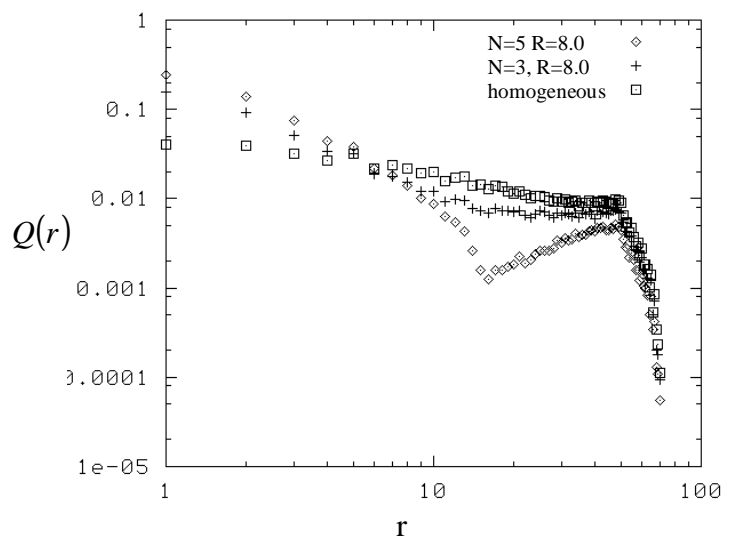
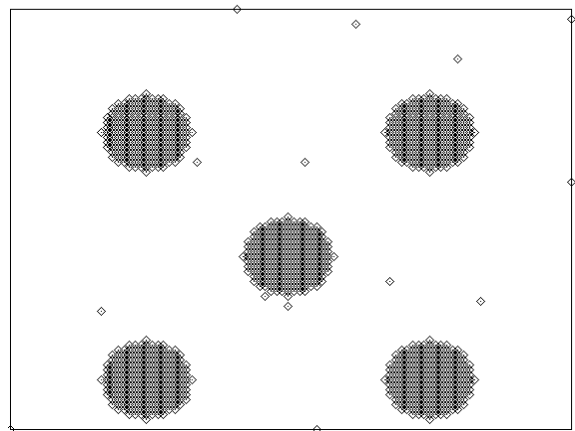
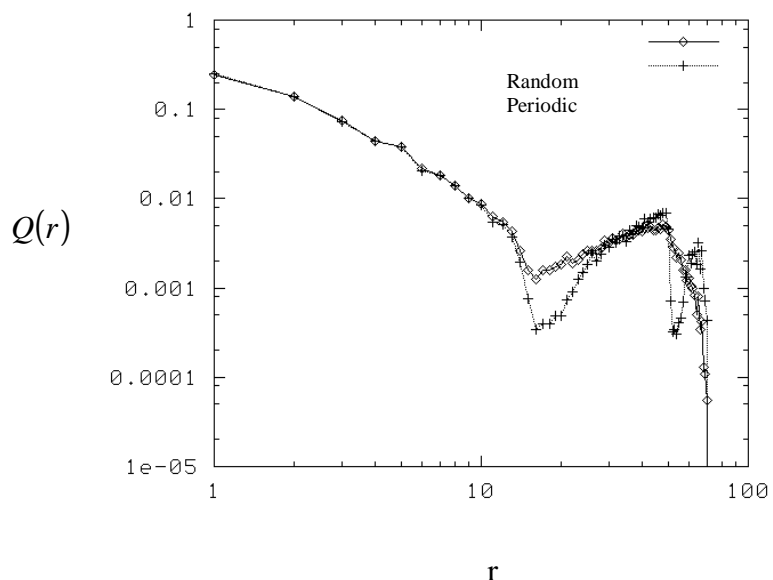


Fig 5

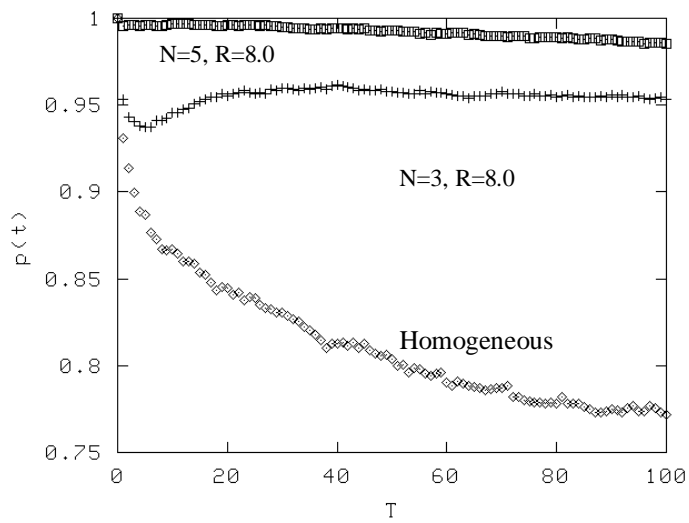


(A)

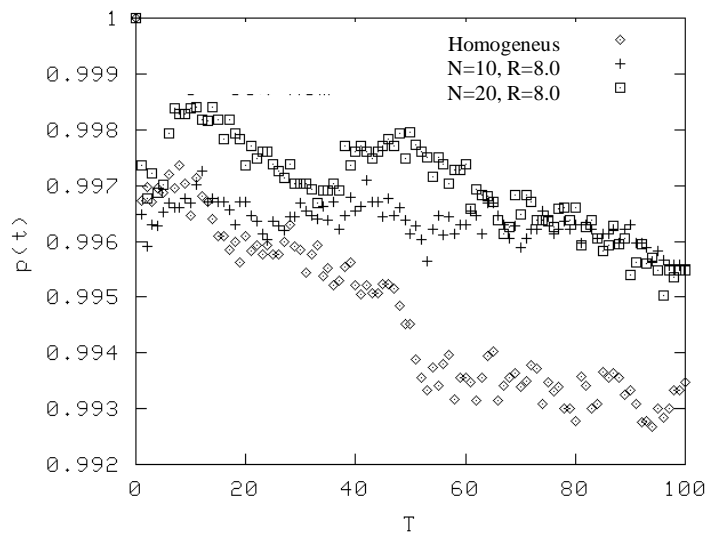


(B)

Fig 6



(A)



(B)

Fig 7